The Journal of Chemical Physics

Global elucidation of broken symmetry solutions to the independent particle model through a Lie algebraic approach

Cite as: J. Chem. Phys. **149**, 194106 (2018); https://doi.org/10.1063/1.5049827
Submitted: 25 July 2018 . Accepted: 26 October 2018 . Published Online: 20 November 2018

Lee M. Thompson

Global elucidation of broken symmetry solutions to the independent particle model through a Lie algebraic approach

Lee M. Thompson[a)]
Department of Chemistry, University of Louisville, Louisville, Kentucky 40205, USA

(Received 25 July 2018; accepted 26 October 2018; published online 20 November 2018)

Broken symmetry solutions—solutions to the independent particle model that do not obey all symmetries required by the Hamiltonian—have attracted significant interest for capturing multireference properties with mean-field scaling. However, identification and optimization of broken-symmetry solutions is difficult owing to the non-linear nature of the self-consistent field (SCF) equations, particularly for solutions belonging to low-symmetry subgroups and where multiple broken symmetry solutions are sought. Linearization of SCF solution space results in the Lie algebra, which this work utilizes as a framework for elucidation of the set of solutions that exist at the desired symmetry. To demonstrate that searches constructed in the Lie algebra yield the set of broken symmetry solutions, a grid-based search of real-restricted, real-unrestricted, complex-restricted, paired-unrestricted, and real-general solutions of the C_{2v} (nearly D_{4h}) H_4 molecule is performed. *Published by AIP Publishing.*
https://doi.org/10.1063/1.5049827

I. INTRODUCTION

The many-electron Hamiltonian places constraints on the permitted symmetries of the corresponding eigenfunctions. However, within a mean-field formalism, solutions that do not contain all the required symmetries have variational freedom to potentially obtain improved energies. While symmetry breaking is an artefact resulting from approximations underlying mean-field solutions, it captures to an extent the energy contributions that arise from strongly correlated electrons. Broken symmetry solutions have been used as first-order wavefunctions in several theoretical approaches,[1–5] as well as in their own right to explore a broad range of chemical problems through density functional theory (DFT). However, difficulties are encountered in obtaining the desired broken symmetry solution and there are relatively few general methods for systematically elucidating the multiple different broken symmetry solutions.[6,7] This article demonstrates that utilizing the Lie algebra that describes properties of the unitary group, elucidation of solutions of a desired symmetry can be obtained through a deterministic search of wavefunction parameter space.

Despite technical difficulties in obtaining broken symmetry solutions and debate regarding their validity, they have in fact been used widely in chemical simulations. However, broken symmetry solutions are almost always used in the guise of real unrestricted (RU) calculations where complex-conjugation and S_z spin symmetries are preserved. The reason for the widespread utilization of RU approaches is that they describe diradical and antiferromagnetic systems, and thus identification of solutions is facilitated through chemical intuition. However, RU represents one class of broken symmetry solution[8] and the other classes have not seen widespread application outside of a small number of research groups.[9,10]

Typically RU solutions are determined by local optimization of an initial guess generated from mixing α and β frontier orbitals, or in more complicated molecules through a fragment guess approach. Stability analysis can reveal optimization directions that further break the spin symmetry,[11,12] and the orbital rotation Hessian can be used to perform a further local optimization or even to find a globally optimum solution.[13] However, for some applications, it is desirable to obtain a complete understanding of the mean-field solutions available at a given geometry, for example in cases where there are several low-lying broken symmetry solutions,[14,15] for use as diabats in nonadiabatic mechanism studies,[16,17] or as an alternative basis for configuration interaction (CI) calculations.[18] Finding symmetry subgroups other than RU becomes increasingly difficult due to reduced chemical intuition for constructing initial guesses. Furthermore, global elucidation of mean-field wavefunction parameter space is complicated by the nonlinear equations of the self-consistent field (SCF) approach which (i) prevents *a priori* knowledge of the number of solutions beyond a set of bounds[19] and (ii) can collapse to low-lying solutions that are not local to the initial guess.

In this article, we describe and apply a grid-based approach for location of multiple solutions to the SCF equations using the unitary group properties of the molecular orbital (MO) coefficients. Using the exponential mapping between the unitary group and the associated Lie algebra, it is possible to linearize certain algebraic properties of matrices which facilitate implementation of solution optimization algorithms. A search of several different broken symmetry solution classes in the C_{2v} (nearly D_{4h}) H_4 molecule is performed using a regular grid constructed in the Lie algebra and mapped back to the

a)Electronic mail: lee.thompson.1@louisville.edu

unitary group space. The search can be limited to contain only a desired symmetry subgroup or search over multiple subgroups simultaneously. While the scaling of the grid-based deterministic scales exponentially with the size of the occupied-virtual (ov) space and so is limited to small molecules, we examine how the number of grid points may be reduced. Furthermore, this work demonstrates that the Lie algebraic approach can successfully locate multiple SCF solutions and thus is likely to be a suitable framework for implementation of alternative search algorithms for global elucidation of SCF solution space.

II. METHODS

A. Lie algebraic characterization of self-consistent field solution space

According to Thouless' theorem,[20] any solution of an independent particle model $|\Psi\rangle$ can be obtained from transformation of another solution $|\Phi\rangle$,

$$|\Psi\rangle = e^{\hat{K}}|\Phi\rangle, \tag{1}$$

where $\hat{K}$ is the $\mathfrak{su}(2N_{\text{orb}})$ Lie algebra that linearizes the special unitary group. $\hat{K}$ can be constructed from orbital excitation operators,

$$E^{q\sigma_2}_{p\sigma_1} = a^{\dagger}_{p\sigma_1} a_{q\sigma_2}, \tag{2}$$

where p, q, r, ... represent MOs, σ_i is the electron spin coordinate which is +1/2 for α spin and −1/2 for β spin, and $a^{\dagger}$ and a are particle creation and annihilation operators, respectively. Using irreducible Cartesian orbital excitation operators [Eq. (A21)] $\hat{K}$ is written as (see Appendix A for further derivation details)

$$\begin{aligned}\hat{K} = i\sum_{p}[k^{D,00}_{pp}S^{00}_{pp} + \sum_{x_1,x_2,x_3} k^{D,x_i}_{pp}T^{x_i}_{pp}] + i\sum_{p>q}[k^{S,00}_{pq}(S^{00}_{pq} + S^{00}_{qp}) \\ + \sum_{x_1,x_2,x_3} k^{S,x_i}_{pq}(T^{x_i}_{pq} + T^{x_i}_{qp})] + \sum_{p>q}[k^{A,00}_{pq}(S^{00}_{pq} - S^{00}_{qp}) \\ + \sum_{x_1,x_2,x_3} k^{A,x_i}_{pq}(T^{x_i}_{pq} - T^{x_i}_{qp})].\end{aligned} \tag{3}$$

In the notation used here, each generator is distinguished by its superscript indicating whether it is from the symmetric or antisymmetric partition and the Cartesian basis vector to which it belongs. To construct a wavefunction belonging to a particular subgroup, $\hat{K}$ (where $\hat{K} = \sum \hat{k}$) is built with only generators $\hat{k}$ that are invariant to the relevant symmetry operations. The set of MOs which in an orthonormal basis form an element of $SU(2N_{\text{orb}})$ is then obtained through exponential mapping, as described in Appendix B.

An approach to establish the invariance of the generators is to study the structure of the matrix representation in the spin-blocked form. Generators $\hat{k}$ are invariant upon action of a symmetry operator $\hat{g}$ which is an element of a symmetry group G if the matrix remains unchanged after action of the symmetry operation according to

$$[\hat{g}, \hat{k}] = 0 \Leftrightarrow \hat{g}\hat{k}\hat{g}^{-1} = \hat{k} \qquad (\forall \hat{g} \in G). \tag{4}$$

Using Eqs. (3) and (4) and the matrix representation of E^{p}_{q}, the matrix representations of the 8 possible ov generators are

$$\mathbf{k}^{A,00} = ik^{A,00}\begin{bmatrix}\boldsymbol{\sigma}^{pq}_{y} & \mathbf{0}\\ \mathbf{0} & \boldsymbol{\sigma}^{pq}_{y}\end{bmatrix}, \tag{5}$$

$$\mathbf{k}^{S,00} = ik^{S,00}\begin{bmatrix}\boldsymbol{\sigma}^{pq}_{x} & \mathbf{0}\\ \mathbf{0} & \boldsymbol{\sigma}^{pq}_{x}\end{bmatrix}, \tag{6}$$

$$\mathbf{k}^{A,z} = ik^{A,z}\begin{bmatrix}\boldsymbol{\sigma}^{pq}_{y} & \mathbf{0}\\ \mathbf{0} & -\boldsymbol{\sigma}^{pq}_{y}\end{bmatrix}, \tag{7}$$

$$\mathbf{k}^{S,z} = ik^{S,z}\begin{bmatrix}\boldsymbol{\sigma}^{pq}_{x} & \mathbf{0}\\ \mathbf{0} & -\boldsymbol{\sigma}^{pq}_{x}\end{bmatrix}, \tag{8}$$

$$\mathbf{k}^{A,x} = ik^{A,x}\begin{bmatrix}\mathbf{0} & \boldsymbol{\sigma}^{pq}_{y}\\ \boldsymbol{\sigma}^{pq}_{y} & \mathbf{0}\end{bmatrix}, \tag{9}$$

$$\mathbf{k}^{S,x} = ik^{S,x}\begin{bmatrix}\mathbf{0} & \boldsymbol{\sigma}^{pq}_{x}\\ \boldsymbol{\sigma}^{pq}_{x} & \mathbf{0}\end{bmatrix}, \tag{10}$$

$$\mathbf{k}^{A,y} = k^{A,y}\begin{bmatrix}\mathbf{0} & \boldsymbol{\sigma}^{pq}_{y}\\ -\boldsymbol{\sigma}^{pq}_{y} & \mathbf{0}\end{bmatrix}, \tag{11}$$

$$\mathbf{k}^{S,y} = k^{S,y}\begin{bmatrix}\mathbf{0} & \boldsymbol{\sigma}^{pq}_{x}\\ -\boldsymbol{\sigma}^{pq}_{x} & \mathbf{0}\end{bmatrix}, \tag{12}$$

where $\boldsymbol{\sigma}^{pq}_{x}$ and $\boldsymbol{\sigma}^{pq}_{y}$ are Pauli matrices over orbitals p, q (with all elements other than p, q and q, p equal to zero).

Inspection of the Hamiltonian demonstrates that a many-electron system is invariant to spin rotations and time reversal. Spin rotations form an isomorphism with the $SU(2)$ group, while time reversal is described by the four element finite group $\{\pm\hat{1}, \pm\hat{\Theta}\}$. The spin rotation operators $\{\hat{S}_x, \hat{S}_y, \hat{S}_z\}$ can be expressed using the generators of the $SU(2)$ group ($\hat{s}$) which are constructed using Pauli spin matrices. In terms of excitation operators, each spin rotation operator can be written as

$$\hat{S}_x = \frac{1}{2}\boldsymbol{\sigma}^{pq}_{x}, \tag{13}$$

$$\hat{S}_y = -\frac{1}{2}\boldsymbol{\sigma}^{pq}_{y}, \tag{14}$$

$$\hat{S}_z = \frac{1}{2}\boldsymbol{\sigma}^{pq}_{x}. \tag{15}$$

The $SU(2)$ generators are $\hat{s}_w = \exp(i\hat{S}_w\theta)$ for $w = \{x, y, z\}$. Similarly the time reversal operator can be written as

$$\hat{\Theta} = \exp(-i\pi\hat{S}_y)\hat{C}, \tag{16}$$

where $\hat{C}$ is the complex conjugation operator.

The action of symmetry operations [Eqs. (13)–(16)] on the generators $\hat{k}$ can be established by consideration of transformation on the underlying creation and annihilation operators,[21]

$$\begin{aligned}\exp(i\hat{S}_x\theta)E^{q\sigma_2}_{p\sigma_1}\exp(-i\hat{S}_x\theta) = \frac{1}{2}(E^{q\sigma_2}_{p\sigma_1} + E^{q(-\sigma_2)}_{p(-\sigma_1)}) \\ + \frac{1}{2}\cos(\theta)(E^{q\sigma_2}_{p\sigma_1} - E^{q(-\sigma_2)}_{p(-\sigma_1)}) \\ + \frac{i}{2}\sin(\theta)(E^{q(-\sigma_2)}_{p\sigma_1} + E^{q\sigma_2}_{p(-\sigma_1)}),\end{aligned} \tag{17}$$

$$\begin{aligned}\exp(i\hat{S}_z\theta)E^{q\sigma_2}_{p\sigma_1}\exp(-i\hat{S}_z\theta) = \delta_{\sigma_1\sigma_2}E^{q\sigma_2}_{p\sigma_1} + \delta_{\sigma_1(-\sigma_2)} \\ \times \exp(i\theta\,\text{sign}(\sigma_1))E^{q\sigma_2}_{p\sigma_1},\end{aligned} \tag{18}$$

TABLE I. Invariance of generators of $\hat{K}$.

Generator	Invariant	Not invariant
$\hat{k}^{A,00}$	$\hat{S}^2, \hat{S}_z, \hat{\Theta}, \hat{C}, \hat{1}$	
$\hat{k}^{S,00}$	$\hat{S}^2, \hat{S}_z, \hat{1}$	$\hat{\Theta}, \hat{C}$
$\hat{k}^{A,z}$	$\hat{S}_z, \hat{C}, \hat{1}$	$\hat{S}^2, \hat{\Theta}$
$\hat{k}^{S,z}$	$\hat{S}_z, \hat{\Theta}, \hat{1}$	$\hat{S}^2, \hat{C}$
$\hat{k}^{A,x}$	$\hat{C}, \hat{1}$	$\hat{S}^2, \hat{S}_z, \hat{\Theta}$
$\hat{k}^{S,x}$	$\hat{\Theta}, \hat{1}$	$\hat{S}^2, \hat{S}_z, \hat{C}$
$\hat{k}^{A,y}$	$\hat{1}$	$\hat{S}^2, \hat{S}_z, \hat{\Theta}, \hat{C}$
$\hat{k}^{S,y}$	$\hat{\Theta}, \hat{C}, \hat{1}$	$\hat{S}^2, \hat{S}_z$

$$\hat{C}(cE^{q\sigma_2}_{p\sigma_1})\hat{C} = c^* E^{q\sigma_2}_{p\sigma_1}, \tag{19}$$

$$\hat{\Theta}(cE^{q\sigma_2}_{p\sigma_1})\hat{\Theta}^{-1} = c^*(-1)^{\sigma_1+\sigma_2-1} E^{q(-\sigma_2)}_{p(-\sigma_1)}, \tag{20}$$

where $c \in \mathbb{C}$. Applying these rules to the generators $\hat{k}$ reveals which symmetry operations the generators are invariant to (Table I). Grouping together generators that are invariant to each symmetry operation reveals the different classes of SCF solutions (Table II) and gives rise to the eight groups identified by Fukutome[8] as well as one further symmetry group, designated real-paired general (RPG). However, RPG solutions are collinearly aligned with the y axis and can be transformed into paired unrestricted (PU) solutions through spin rotation (the spin rotation operator does not commute with the complex conjugation operator). The spin rotational axes are not well defined in the absence of spin-orbit coupling or magnetic fields and so RPG is not a distinct symmetry group, as is clear from inspection of the MO coefficients and density matrix of PU and RPG solutions,

$$\mathbf{C}_{\mathrm{PU}} = \begin{bmatrix} \mathbf{A} & \mathbf{0} \\ \mathbf{0} & \mathbf{A}^* \end{bmatrix} \quad \mathbf{P}_{\mathrm{PU}} = \begin{bmatrix} \mathbf{A}\mathbf{A}^\dagger & \mathbf{0} \\ \mathbf{0} & \mathbf{A}^*\mathbf{A}^\intercal \end{bmatrix} = \begin{bmatrix} \mathbf{E} & \mathbf{0} \\ \mathbf{0} & \mathbf{E}^\intercal \end{bmatrix} \quad (A_{ij}, E_{ij} \in \mathbb{C}), \tag{21}$$

$$\mathbf{C}_{\mathrm{RPG}} = \begin{bmatrix} \mathbf{A} & \mathbf{B} \\ -\mathbf{B} & \mathbf{A} \end{bmatrix}, \quad \mathbf{P}_{\mathrm{RPG}} = \begin{bmatrix} \mathbf{A}\mathbf{A}^\intercal + \mathbf{B}\mathbf{B}^\intercal & \mathbf{B}\mathbf{A}^\intercal - \mathbf{A}\mathbf{B}^\intercal \\ \mathbf{A}\mathbf{B}^\intercal - \mathbf{B}\mathbf{A}^\intercal & \mathbf{A}\mathbf{A}^\intercal + \mathbf{B}\mathbf{B}^\intercal \end{bmatrix} = \begin{bmatrix} \mathbf{E} & \mathbf{F} \\ -\mathbf{F} = \mathbf{F}^\intercal & \mathbf{E} \end{bmatrix} \quad (A_{ij}, B_{ij}, E_{ij}, F_{ij} \in \mathbb{R}), \tag{22}$$

where owing to the hermiticity of the density matrix, Re(**E**) is the same in both Eqs. (21) and (22), while Im(**E**) in Eq. (21) is equal to Re(**F**) in Eq. (22).

To provide some insight as to the action of generators, we briefly highlight the role of $\mathbf{K}^{A,00}_{12}$ and $\mathbf{K}^{S,00}_{12}$ acting on the real restricted (RR) ground state of H_2, where orbitals 1 and 2 are the bonding and antibonding orbitals, respectively. $\mathbf{K}^{A,00}_{12}$ would produce solutions with orbitals that break $D_{\infty h}$ symmetry but preserve real orbital coefficients and alpha-beta orbital equivalence. $\mathbf{K}^{S,00}_{12}$ will preserve $D_{\infty h}$ symmetry and alpha-beta orbital equivalence but produce complex valued orbitals. Application of both generators simultaneously will break $D_{\infty h}$ symmetry and complex-conjugation symmetry but preserve alpha-beta orbital equivalence. Solutions with both broken spatial and complex-conjugation symmetries can only be accessed through application of both generators simultaneously.

B. Global search of wavefunction parameter space using Lie algebraic approach

Through the derivation in Sec. II A, searches across wavefunction parameter space can be performed in a linearized Lie algebra which can be mapped back to the non-linear group manifold. One approach is to construct a regular grid of points in the linearized vector space that perform non-trivial changes to the Slater determinant and map these back to the group to generate a number of initial guesses which are then optimized through an SCF procedure to a local minimum. While such an approach is limited to small systems due to exponential scaling of grid based searches with dimensionality of the vector space, our aim is to demonstrate that construction of search algorithms in the linearized vector space can be successfully used for global elucidation of SCF solutions.

Figure 1 demonstrates how grid points in the Lie algebra (red) appear after being mapped to the *SU* group manifold (blue). The Lie algebra is formed from the tangent space of the original solution which lies on the z axis, and grid points are mapped from the Lie algebra to the Lie group manifold through Eq. (B1). Truncation of Eq. (B1) at second order results in some small deviations of grid points on the group manifold from their correct positions; however, the deviations are only apparent at larger rotation angles and should not

TABLE II. Wavefunction symmetries constructed from generators $\hat{K}$.

Wavefunction class	Preserved symmetries	Generators
Real restricted (RR)	$\hat{S}^2, \hat{S}_z, \hat{\Theta}, \hat{C}, \hat{1}$	$\hat{k}^{A,00}$
Complex restricted (CR)	$\hat{S}^2, \hat{S}_z, \hat{1}$	$\hat{k}^{A,00} + \hat{k}^{S,00}$
Real unrestricted (RU)	$\hat{S}_z, \hat{C}, \hat{1}$	$\hat{k}^{A,00} + \hat{k}^{A,z}$
Paired unrestricted (PU)	$\hat{S}_z, \hat{\Theta}, \hat{1}$	$\hat{k}^{A,00} + \hat{k}^{S,z}$
Complex unrestricted (CU)	$\hat{S}_z, \hat{1}$	$\hat{k}^{A,00} + \hat{k}^{S,00} + \hat{k}^{A,z} + \hat{k}^{S,z}$
Real general (RG)	$\hat{C}, \hat{1}$	$\hat{k}^{A,00} + \hat{k}^{A,z} + \hat{k}^{A,x} + \hat{k}^{S,y}$
Complex-paired general (CPG)	$\hat{\Theta}, \hat{1}$	$\hat{k}^{A,00} + \hat{k}^{S,z} + \hat{k}^{S,x} + \hat{k}^{S,y}$
Complex general (CG)	$\hat{1}$	$\hat{k}^{A,00} + \hat{k}^{S,00} + \hat{k}^{A,z} + \hat{k}^{S,z} + \hat{k}^{A,x} + \hat{k}^{S,x} + \hat{k}^{A,y} + \hat{k}^{S,y}$
Real-paired general (RPG)	$\hat{\Theta}, \hat{C}, \hat{1}$	$\hat{k}^{A,00} + \hat{k}^{S,y}$

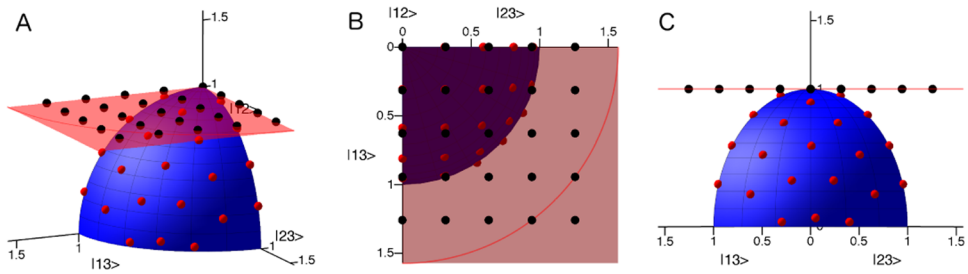

FIG. 1. (a) Illustration of relation of the Lie algebra vector space (red) and the *SU* group manifold (blue) for the case of a two electron in three orbital system. The initial set of molecular orbital coefficients lie on the z axis and correspond to the $|12\rangle$ eigenstate. (b) Generation of regular grid in the Lie algebra vector space where the red line shows set of points with vector norm $\pi/2$ beyond which grid points can be discarded. (c) Grid points mapped to the unitary group manifold through Zassenhaus' formula up to the second order.

significantly affect the search as rotations beyond $\pi/2$ are not used. Where finer grids are used, some of the generated grid points may lie further than $\pi/2$ away from the origin, as indicated by the red line in Fig. 1(b), and so can be discarded. Although the grid on the *SU* manifold appears reasonably well-spaced (especially at smaller rotation angles), alternatives approaches may give better distribution.[22,23] However, the regular grid approach is easily generalized to arbitrary dimensions necessary for electronic structure problems.

Unfortunately, as is typical of grid-based approaches, the number of grid points grows very large as the size of the vector space increases. The number of initial guesses N_{guess} generated by such a grid-based scheme is

$$N_{\text{guess}} = N_{\text{grid}}^{(N_{\text{gen}} \times N_{\text{ov}})}, \tag{23}$$

where N_{grid} is the number of grid points along each basis vector, N_{gen} is the number of generators for the chosen symmetry (Table II), and N_{ov} is the number of elements in the ov space. Even though performing an SCF optimization on each grid point is completely independent and thus the procedure is highly parallelized, the number of initial guesses grows prohibitively large very quickly. Thus it is necessary to develop approaches for selecting the relevant subspace over which to search to generate a tractable grid-based approach.

Examining Eq. (23), it is clear that there are three ways to reduce the number of generated initial solutions—reduce the number of grid points, reduce the number of generators, reduce the size of the ov space, or some combination of these three.

The number of grid points defines how fine the search grid is along a given basis vector. While in principle this could be an arbitrarily large number, in reality the minimum number of N_{grid} is related to the number of minima in SCF space along that basis vector. N_{grid} defines the different values of k, where 0 leaves the orbitals unchanged, $\frac{\pi}{4}$ swaps a pair of orbitals, and values in between correspond to different levels of orbital mixing. Thus each orbital is most different from either of the two starting orbitals around $\frac{\pi}{8}$, and if symmetry breaking is desirable, it would be expected that such a rotation would result in probably only one and most likely not more than two or three minimum along the basis vector. Thus, it is expected that typically N_{grid} can generally be set to a small number. Furthermore, there is no reason to have the same number of grid points along every basis vector and directions that are considered to have more solutions can be set with a larger number of grid points than the remaining directions.

The number of generators defines which symmetries are being broken. However, the generators listed in Table II search not only over the given symmetry subgroup but also over all overgroups. For example, the search for complex restricted (CR) solutions requires generators $\hat{k}^{A,00} + \hat{k}^{S,00}$, but $\hat{k}^{A,00}$ searches over all RR solutions, while $\hat{k}^{S,00}$ searches over all CR solutions around a given RR solution. Therefore, the number of generators can be reduced by performing searches along the subgroup tree (Fig. S1) around desired solutions of the preceding overgroup. Following the above example, one could perform a global RR search to find the lowest energy RR solution (or few lowest energy solutions) and then use that as input to the CR search using only the $\hat{k}^{S,00}$ generator.

The size of the ov space can be reduced by searching over a subset of orbitals. To obtain an orbital subset, a user selected active space is defined containing orbitals which are likely to contribute to broken symmetry solutions. While such an approach requires a level of chemical intuition and results in a method that is no longer strictly black box, it may be combined with tests to indicate where solutions lie outside of the chosen active space.[13] Within the defined orbital active space, the number of ov rotations can be further reduced by constraining the number of orbital rotations for each initial guess. The total number of initial guesses generated can be written in terms of the number of orbital rotations N_{rot} as

$$N_{\text{guess}} = \sum_{N_{\text{rot}}=0}^{N_{\text{gen}} \times N_{\text{ov}}} \binom{N_{\text{gen}} \times N_{\text{ov}}}{N_{\text{rot}}} \times (N_{\text{grid}} - 1)^{N_{\text{rot}}}. \tag{24}$$

When $N_{\text{rot}} = 0$, the rotation matrix is the identity and the generated guess will be the same as the initial guess. Therefore, the lowest rotation level of N_{rot} should be 1. If N_{grid} can be limited to two (including the grid point at the origin), then the number of initial guesses per orbital rotation level does not scale with the number of grid points and it is feasible to include higher order rotations. However, in the case that $N_{\text{gen}} \times N_{\text{ov}}$ is large, a large number of initial guesses will be generated. However, the orbital rotations have analogy with Slater determinant substitutions in CI approaches (this is how broken symmetry solutions capture correlation effects[24]) and so lower-order orbital

rotations will be most important. By restricting the order of orbital rotation, far more manageable numbers of initial guesses can be generated.

Starting from the set of initial points, standard SCF optimization techniques can be used to find relevant minima. However, direct inversion of the iterative subspace (DIIS) based approaches will miss many solutions as the wavefunction can be optimized to a non-local solution. To avoid this problem, the initial maximum overlap method (IMOM) algorithm[25] can be used to elucidate all SCF solutions that are local to the set of initial guesses. The global search algorithm is summarized as follows, making use of the efficiency considerations discussed:

1. Locate a SCF solution of a particular symmetry.
2. Determine the symmetry subgroup from which global solutions should be obtained.
3. Select the active space of orbitals which are believed to contain the important correlations.
4. Select the number of grid points for each basis vector and number of ov rotations.
5. Construct a regular grid over selected basis vectors.
6. Perform the exponential mapping back to the group manifold to obtain the set of rotation matrices.
7. Apply rotation matrices to solution MOs from step 1 to obtain set of guess MOs.
8. Starting from the set of guess MOs, perform SCF optimization.

III. NUMERICAL RESULTS

To illustrate the utility of the approach in Sec. II B, calculations are performed on H_2 and H_4 to elucidate the various SCF solutions present. The set of initial MO coefficient guesses were generated using an in-house code which makes use of the MQCPack library.[26] Initial guess solutions were then optimized using a modified version of Gaussian 16.[27]

A. H_2 dissociation

The location of broken symmetry solutions along the H_2 dissociation profile is shown in Fig. 2 alongside the full configuration interaction (FCI) curves computed in the Slater determinant basis. At the dissociation limit, six different broken symmetry solutions were located (not accounting for degeneracies), which coalesce into four solutions at the ground state equilibrium geometry. The lowest energy solution corresponds to the well-known RU solutions which split from the RR solution at the Coulson-Fischer point. At dissociation, the lowest energy singlet RU solution is degenerate with a collinear triplet state obtained by breaking the $\hat{S}_z$ symmetry to form a real general (RG) initial guess. Upon optimization, the triplet state is obtained by performing a spin flip, resulting in six degenerate solutions characterized by a ± 1 $\langle \hat{S}_x \rangle$, $\langle \hat{S}_y \rangle$, or $\langle \hat{S}_z \rangle$ expectation value. As the high spin state can be written exactly as a single determinant, the triplet state is the same energy as that obtained from FCI.

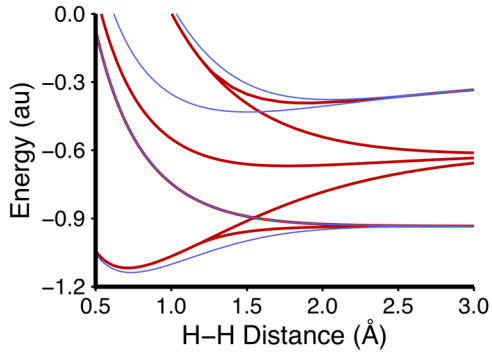

FIG. 2. Location of broken symmetry Hartree-Fock STO-3G solutions of the H_2 molecule (red) compared to full configuration interaction STO-3G solutions (blue).

The lowest energy RR solution only captures ionic components of the wavefunction and so climbs above the singlet and triplet RU solutions to become degenerate with two higher energy curves. Of the two curves to which the RR solution is degenerate, the lower energy at the ground-state equilibrium geometry corresponds to a singly substituted RU solution that preserves the spatial symmetry (α and β orbitals differ, but the orbitals are irreducible representations of the nuclear point group). The other curve which is at higher energy at the ground-state equilibrium geometry is a doubly substituted RR solution which preserves the spatial symmetry and is internally stable. At short distances, the spatially symmetric RR solution coalesces with a second internally unstable RR solution that breaks the spatial symmetry. At the dissociation limit, the spatially broken RR solution is identical with the FCI results that correspond to the singly excited and doubly excited states.

B. H_4 trapezoid

Turning to H_4, we seek to understand how truncation of the Lie algebra vector space affects the solutions that can be determined. Furthermore, previous approaches for elucidating the full RR SCF solution space have made use of this system.[6,7] Calculations with Huzinaga's minimal basis set[28] were performed using a C_{2v} trapezoid geometry with H_1–H_2, H_2–H_3, and H_3–H_4 bond distances set to 2.0 a_0 and H_1–H_2–H_3 and H_2–H_3–H_4 angles set to 90.9°. Table III illustrates the RR solutions found as a function of grid points along each basis vector as well as permitted number of orbital rotations. In the derivation of Sec. II A, there is no attempt to take account of the point group symmetry and thus we expect to find all solutions regardless of spatial symmetry breaking.

All 13 previously identified RR solutions were located using four grid points along each basis vector. However, even with one grid point, the six lowest-energy solutions were identified, while two and three grid points were able to identify ten and eleven solutions, respectively, suggesting that tighter grids are required only for the higher-energy pathologically behaved solutions. Indeed, all the solutions identified with one grid point can be found at all geometries in which the H_1–H_2–H_3 and H_2–H_3–H_4 angles are increased to break quasi-degeneracy. Similarly, all solutions were obtained from initial guesses generated with up to three orbital rotations, while most solutions were found with a limit of one or two orbital

TABLE III. Stationary solutions to the H_4 real-restricted Hartree-Fock equations located as a function of grid points along each basis vector and maximum orbital rotation number.

		Minimum rotation # required with grid points			
Solution #	Energy (a.u.)	1	2	3	4
1	−1.871 397	1	1	1	1
2	−1.851 306	1	1	1	1
3	−1.815 135	2	3	2	1
4	−1.032 896	3	1	1	1
5	−0.820 861	2	1	1	1
6	−0.148 480	1	1	1	1
7	−0.133 029		2	3	2
8	−0.132 914		2	2	2
9	−0.123 536				3
10	−0.123 495			3	3
11	−0.117 115			3	3
12	−0.116 207		3	3	2
13	−0.093 966		2	2	2

rotations. A general trend is that solutions are located at a lower orbital rotation limit when there are a greater number of grid points. In agreement with the previous studies, of the solutions found, only solutions 1 and 2 were internally stable, five solutions were spatial symmetry-broken RR symmetry solutions, while the remainder preserved the spatial symmetry as all orbitals corresponded to an irreducible representation of the molecular point group.

To test the methodology for locating lower-symmetry solutions, an evaluation of H_4 RU solutions was performed (Table IV). A simultaneous search of RU and RR solutions using both $\hat{k}^{A,00}$ and $\hat{k}^{A,z}$ generators with two grid points and up to four orbital rotations obtained all the solutions listed in Table IV and all RR solutions in Table III. Even with only one grid point, all RU solutions were obtained, along with RR solutions 1–6 and 13. To explore which solutions can be obtained by searching only in the local region of each RR solution, a search of RU space was performed with four grid points using each RR solution as an initial guess and excluding transformations resulting from action of $\hat{k}^{A,00}$. All RU solutions were found to be local to at least two RR solutions, and 17 RU solutions could be obtained directly from seven or more RR solutions. While increasing the number of grid points may enable more solutions to be located, it appears that some solutions are not in the vicinity of a particular RR solution and so cannot ever be found from a local search. For example, RU solution 2 could not be obtained from a search around RR solution 1, even when ten grid points were used. Of the solutions identified, only solution 1 was internally stable.

Examination of CR and PU solutions including the $\hat{k}^{A,00}$ generator with one grid point revealed both symmetries to have solutions at −1.874 915 and −0.153 315 a.u. The overlaps of the different solutions were $\langle \Psi_{\mathrm{PU}}^{-1.87} | \Psi_{\mathrm{CR}}^{-1.87} \rangle = 0.19 - 0.40i$ and $\langle \Psi_{\mathrm{PU}}^{-0.15} | \Psi_{\mathrm{CR}}^{-0.15} \rangle = 0.12 - 0.33i$. The CR solution is distinct and degenerate to the PU solution, with each preserving a different set of symmetries. The comparison of CR MO coefficients and density matrix

TABLE IV. Real-unrestricted solutions to the Hartree-Fock equations for H_4 with list of real-restricted solutions from which each solution can be obtained without rotating through a second real-restricted solution.

Solution #	Energy (a.u.)	Real-restricted initial solution #
1	−1.961 129	1, 2, 6, 7, 8, 9, 10, 11, and 12
2	−1.884 030	3, 7, 10, 12, and 13
3	−1.464 491	1, 3, 4, 7, 9, 10, 11, 12, and 13
4	−1.464 488	3, 4, 5, 7, 8, 9, 10, 11, 12, and 13
5	−1.454 348	3, 7, 8, 9, 10, 11, 12, and 13
6	−1.357 439	3, 4, 7, 8, 9, 10, 11, and 12
7	−1.347 041	1, 5, 7, 8, 9, 10, 11, 12 and 13
8	−1.084 510	1, 2, 6, 7, 8, 9, 10, 11, and 12
9	−1.043 560	9, 10, 11, 12, and 13
10	−1.040 975	3, 7, 9, and 13
11	−1.028 540	5, 7, 8, 9, 10, 11, and 12
12	−1.010 631	4, 7, 8, 9, 10, 11, and 12
13	−0.973 265	3, 7, 9, 10, 11, 12 and 13
14	−0.932 281	9 and 11
15	−0.601 683	3, 5, 7, 9, 10, 11, 12, and 13
16	−0.593 935	1, 3, 5, 7, 9, 10, 11, 12, and 13
17	−0.593 739	3, 9, 10, 11, 12, and 13
18	−0.496 879	3, 4, 7, 9, 10, 11, and 12
19	−0.488 922	1, 3, 4, 8, 9, 10, 11, and 12
20	−0.488 762	1, 3, 7, 8, 9, 10, 11, 12 and 13
21	−0.186 906	1, 2, 6, 7, 8, 9, 10, 11, 12, and 13
22	−0.163 297	3, 7, 9, 10, 11, 12, and 13

$$\mathbf{C}_{\mathrm{CR}} = \begin{bmatrix} \mathbf{A} & \mathbf{0} \\ \mathbf{0} & \mathbf{A} \end{bmatrix}, \quad \mathbf{P}_{\mathrm{CR}} = \begin{bmatrix} \mathbf{A}\mathbf{A}^{\dagger} & \mathbf{0} \\ \mathbf{0} & \mathbf{A}\mathbf{A}^{\dagger} \end{bmatrix} = \begin{bmatrix} \mathbf{E} & \mathbf{0} \\ \mathbf{0} & \mathbf{E} \end{bmatrix} \quad (A_{ij}, E_{ij} \in \mathbb{C}) \tag{25}$$

with Eq. (21) demonstrates that **E** in both solutions is identical, and the expected structure of the density matrix is observed in both PU and CR solutions. Testing of the CR and PU density matrix[29] confirmed that the CR solution did indeed have restricted character, while the PU solution was collinear.

Finally, a RG search using generators $\hat{k}^{A,00}$, $\hat{k}^{A,z}$, $\hat{k}^{A,x}$, and $\hat{k}^{S,y}$ to simultaneously search over RR and RU solutions was performed using RR state 1 as the initial guess with one grid point (see Table S1 for full results). The search located all RR and RU solutions, except for RR solutions 9, 10, 11, and 12. As established in Table III, the location of RR solutions 9, 10, 11, and 12 likely requires a finer grid. In addition to the solutions located with RU and RR symmetries, a further 31 RG solutions were obtained (not counting multiplicity). Of the 31 RG solutions, 21 were triplet solutions, in which optimization in the RG framework had allowed a single spin flip. In fact the lowest energy RG solution, with energy −1.941 379 a.u., corresponded to such a triplet state. In addition, the quintet solution at −1.388 326 a.u. was identified, leaving a total of 8 noncollinear (but coplanar owing to the constraints of RG symmetry) solutions. The lowest energy noncollinear solution has energy −1.087 998 a.u. As indicated by the vector field shown in Fig. 3, the solution has magnetic field orientated in the *xz* plane resulting from the collinear nature of RG solutions (where the z axis is perpendicular to the plane of the H atoms and the x axis is orientated vertically). The magnetic

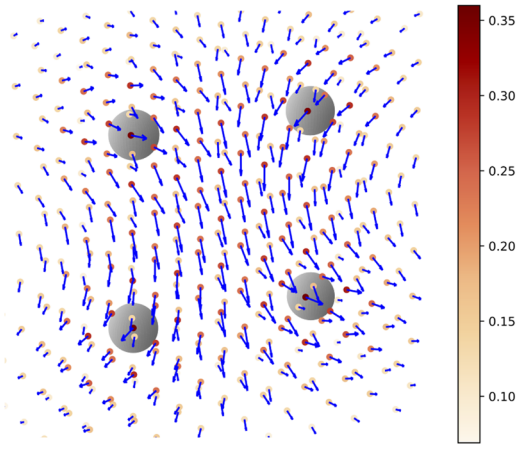

FIG. 3. Magnetic field generated by electron spin in the lowest energy H_4 real general solution at −1.087 998 a.u. Vector direction indicates orientation, and vector length indicates magnitude of the magnetic field. Colored points at vector origin show numerical value of the vector field magnitude.

field is orientated entirely along the $+z$ axis with equal magnitude at top left and bottom right atoms. The top right and bottom left atoms have equal magnetic field orientated with a contribution along $-z$ and $-x$. Thus, a net magnetic field exists which, passing through the center of the four membered ring, produces magnetization in the $+z/-x$ direction.

IV. CONCLUSIONS

An approach for globally elucidating the set of SCF solutions using the $\mathfrak{su}(2N_{\text{orb}})$ Lie algebra that maps to the set of unitary MO coefficient matrices has been presented. Using a grid-based approach to search for SCF solutions, we have demonstrated that despite the non-linearity of the underlying group manifold, it is possible to successfully use a global search technique in the linearized vector space. The regular grid approach was shown to successfully determine all known RR solutions of a quasi-degenerate trapezoidal structure of H_4, while RU, PU, CR, and RG searches were also performed. Several methods for reducing the cost of a grid based search algorithm were discussed, including the use of active spaces, ov rotation limits, grid coarseness, and local subgroup searches. Calculations on H_4 revealed that rotation limits and local subgroup searches could successfully locate a large set of SCF solutions while simultaneously significantly reducing the number of local optimizations required. Furthermore, it was found that all known RR solutions in H_4 could be found with four or fewer grid points and that all but the most pathological, high-energy solutions could be found with two or fewer grid points.

While a grid-based search was used in this investigation in order to assess the viability of a Lie algebraic approach to perform global searches in SCF space, this work demonstrates more generally that algorithms constructed in the tangent vector space and mapped back to the unitary group surface can successfully globally elucidate SCF solutions. The grid-based search is only suitable for relatively small N_{ov} spaces. For larger systems, such as in transition metal systems where broken symmetry SCF generally proves most useful, alternative search algorithms constructed in a similar vein to the grid-based approach are likely to be suitable. In particular, methods borrowed from protein global optimization applications which use stochastic generation of initial guesses may prove advantageous, with algorithms based on multi-start or basin hopping algorithms having potential. Furthermore, taking advantage of the Lie algebraic framework will enable application of algorithms that do not distort the energy hypersurface in order to locate new minima, which is advantageous as there is no guarantee that solutions on a distorted surface map back onto the original space.[30]

SUPPLEMENTARY MATERIAL

See supplementary material for RG energies of quasi-degenerate trapezoidal H_4 with Huzinaga's minimal basis, subgroup inclusion diagram, and table of anticommutation relations of $\mathfrak{su}(2N_{\text{orb}})$ generators.

ACKNOWLEDGMENTS

We gratefully acknowledge the financial support from the University of Louisville and EVPRI Internal Research Grant from the Office of the Executive Vice President for Research and Innovation. This work was conducted in part using the resources of the University of Louisville's research computing group and the Cardinal Research Cluster.

APPENDIX A: DERIVATION OF $\mathfrak{su}(2N_{\text{orb}})$ LIE ALGEBRA

According to Thouless' theorem,[20] any solution of an independent particle model $|\Psi\rangle$ can be obtained from transformation of another solution $|\Phi\rangle$,

$$|\Psi\rangle = e^{\hat{K}}|\Phi\rangle, \tag{A1}$$

where

$$\hat{K} = \sum_{p\sigma_1 q\sigma_2} k_{p\sigma_1 q\sigma_2} a^\dagger_{p\sigma_1} a_{q_{\sigma_2}} = \sum_{p\sigma_1 q\sigma_2} k_{p\sigma_1 q\sigma_2} E^{p\sigma_1}_{q\sigma_2}. \tag{A2}$$

Here we have used the convention that p, q, r, ... represent MOs, σ is the electron spin coordinate, and $a^\dagger$ and a are particle creation and annihilation operators, respectively. The matrix representation of $a_{q\sigma_2}$ in the basis of spatial orbitals (including vacuum state) is dimension $2N_{\text{orb}} + 1 \times 2N_{\text{orb}} + 1$ and contains a 1 in the $q\sigma_2 + 1$st column, 1st row, and zero for all other elements. Similarly, the matrix representation of $a^\dagger_{p\sigma_1}$ is a matrix of zeros except for a 1 in the $p\sigma_1 + 1$st row, 1st column. Thus the matrix representation of $E^{p\sigma_1}_{q\sigma_2}$ is a $2N_{\text{orb}} \times 2N_{\text{orb}}$ matrix (after dropping the vacuum state basis function) of zeros with 1 in the $q\sigma_2$th column, $p\sigma_1$th row. The matrix representation of $E^{p\sigma_1}_{q\sigma_2}$ is required in order to construct the matrix representation of the generators of the Lie algebra.

A solution $|\Phi\rangle$ can be expressed relative to the vacuum state $|0\rangle$ as $|\Phi\rangle = a^\dagger_{i\sigma_1} a^\dagger_{j\sigma_2} a^\dagger_{k\sigma_3} \ldots |0\rangle$, where i, j, k, ... represent occupied MOs. A second solution $|\Psi\rangle$ can similarly be obtained from the vacuum state according to $|\Psi\rangle = \tilde{a}^\dagger_{i\sigma_1} \tilde{a}^\dagger_{j\sigma_2} \tilde{a}^\dagger_{k\sigma_3} \ldots |0\rangle$, where the set $\{\tilde{a}^\dagger\}$ are different

and not necessarily orthonormal to the set $\{a^\dagger\}$. The two solutions are linked by a similarity transformation of the creation operators obtained from the Baker-Campbell-Hausdorff expansion,

$$\tilde{a}^\dagger_{i\sigma_1}|0\rangle = e^{\hat{K}} a^\dagger_{i\sigma_1} e^{-\hat{K}}|0\rangle = a^\dagger_{i\sigma_1} + [\hat{K}, a^\dagger_{i\sigma_1}] + \frac{1}{2!}[\hat{K},[\hat{K},a^\dagger_{i\sigma_1}]] + \ldots|0\rangle, \quad \text{(A3)}$$

which yields the result

$$\tilde{a}^\dagger_{i\sigma_1}|0\rangle = \sum_{m=0}^{\infty}\frac{1}{m!}\sum_{p\sigma_2} k_{p\sigma_2 i\sigma_1} a^\dagger_{p\sigma_2}|0\rangle = \sum_{p\sigma_2} e^{k_{p\sigma_2 i\sigma_1}} a^\dagger_{p\sigma_2}|0\rangle. \quad \text{(A4)}$$

Thus, for a creation operator $\tilde{a}^\dagger = a^\dagger e^{\mathbf{K}}$ and generally the set of MO coefficients for a particular solution $\tilde{\mathbf{C}}$ can be related to the MO coefficients of a second solution $\mathbf{C}$ according to

$$\tilde{\mathbf{C}} = \mathbf{C}e^{\mathbf{K}}. \quad \text{(A5)}$$

$\mathbf{K}$ defines the form of the new set of MO coefficients, and we seek to express $\mathbf{K}$ such that it can be used to obtain solutions of a desired set of symmetries which are subgroups of the initial solution symmetry.

The set of MO coefficient matrices in an orthonormal basis are unitary matrices. Therefore, the set of matrices $\{\tilde{\mathbf{C}}, \mathbf{C}\}$ belong to the $U(2N_{\text{orb}})$ group and according to the group axioms, $e^{\mathbf{K}}$ must also be a unitary matrix if Eq. (A5) holds. As first expressed by Paldus, the $E^{p\sigma_1}_{q_{\sigma_2}}$ of Eq. (A2) form the generators of the unitary group.[31] Thus, Eq. (A2) defines the Lie algebra $\mathfrak{u}(2N_{\text{orb}})$ with a vector space formed of $E^{p\sigma_1}_{q_{\sigma_2}}$ basis vectors and $\mathbf{K}$ vector components, which is mapped back onto the $U(2N_{\text{orb}})$ group through the exponential function.

For $e^{\mathbf{K}}$ to be a unitary matrix, $\mathbf{K}$ is required to be anti-hermitian and can be decomposed into diagonal $\mathbf{D}$, symmetric $\mathbf{S}$ (with 0 on the diagonal), and antisymmetric $\mathbf{A}$ matrices,

$$\mathbf{K} = i\mathbf{D} + i\mathbf{S} + \mathbf{A}. \quad \text{(A6)}$$

A property of unitary matrices is that the determinant is a complex number with norm $\det(\exp(\mathbf{K})) = e^{i\zeta}$. Resulting from the fact that $\mathbf{A}$ and $\mathbf{S}$ have zero diagonal, $\det(\exp(i\mathbf{S}+\mathbf{A})) = \exp(\text{Tr}(i\mathbf{S}+\mathbf{A})) = 1$, and therefore $\det(\exp(\mathbf{K})) = \det(\exp(i\mathbf{D}))\det(\exp(i\mathbf{S}+\mathbf{A}))$ which defines the product group $U(2N_{\text{orb}}) = U(1) \times SU(2N_{\text{orb}})$. The group $U(1)$ describes the ray (set of different phases) of the wavefunction such that $\langle\Psi|\Psi\rangle = 1$. The phase of the wavefunction is generally not observable except in special cases involving interactions between different states (such as those giving rise to Berry phase[32]). Thus we can choose arbitrarily to work in a projective Hilbert space where $|\Psi\rangle = e^{i\mathbf{D}}|\Psi\rangle$ (i.e., $\mathbf{D} = \mathbf{0}$), and we only need to concern ourselves with the group $SU(2N_{\text{orb}})$ constructed from $\mathbf{S}$ and $\mathbf{A}$ that form the $\mathfrak{su}(2N_{\text{orb}})$ Lie algebra. Although commutators of symmetric and antisymmetric generators can generate diagonal generators, the contribution $\mathbf{D}$ can always be removed by projection.

Writing Eq. (A2) making use of the decomposition in Eq. (A6), we obtain

$$\hat{K} = i\sum_{p\sigma} k^D_{p\sigma p\sigma} E^{p\sigma}_{p\sigma} + i\sum_{p\sigma_1>q\sigma_2} k^S_{p\sigma_1 q\sigma_2}(E^{p\sigma_1}_{q\sigma_2} + E^{q\sigma_2}_{p\sigma_1}) + \sum_{p\sigma_1>q\sigma_2} k^A_{p\sigma_1 q\sigma_2}(E^{p\sigma_1}_{q\sigma_2} - E^{q\sigma_2}_{p\sigma_1}). \quad \text{(A7)}$$

The particle-hole formalism of Fukutome[33] is obtained from Eq. (A7) by decomposing the summations further into occupied-occupied (oo), ov, and virtual-virtual (vv) MO terms and regrouping for each $E^{p\sigma_1}_{q\sigma_2}$,

$$\hat{K} = \hat{\Omega}^{\text{D}} + \hat{\Omega}^{\text{O}} + \hat{\Omega}^{\text{V}} + \hat{\Lambda}, \quad \text{(A8)}$$

$$\hat{\Omega}^{\text{D}} = i\sum_{i\sigma} k^D_{i\sigma i\sigma} E^{i\sigma}_{i\sigma} + i\sum_{a\sigma} k^D_{a\sigma a\sigma} E^{a\sigma}_{a\sigma}, \quad \text{(A9)}$$

$$= \sum_{i\sigma}\omega_{i\sigma i\sigma}E^{i\sigma}_{i\sigma} + \sum_{a\sigma}\omega_{a\sigma a\sigma}E^{a\sigma}_{a\sigma}, \quad \text{(A10)}$$

$$\hat{\Omega}^{\text{O}} = \sum_{i\sigma_1>j\sigma 2}(k^A_{i\sigma_1 j\sigma_2} + ik^S_{i\sigma_1 j\sigma_2})E^{j\sigma_2}_{i\sigma_1} - (k^A_{i\sigma_1 j\sigma_2} - ik^S_{i\sigma_1 j\sigma_2})E^{i\sigma_1}_{j\sigma_2}, \quad \text{(A11)}$$

$$= \sum_{i\sigma_1>j\sigma 2}\omega_{i\sigma_1 j\sigma_2}E^{j\sigma_2}_{i\sigma_1} - \omega^*_{i\sigma_1 j\sigma_2}E^{i\sigma_1}_{j\sigma_2}, \quad \text{(A12)}$$

$$\hat{\Omega}^{\text{V}} = \sum_{a\sigma_1>b\sigma 2}(k^A_{a\sigma_1 b\sigma_2} + ik^S_{a\sigma_1 b\sigma_2})E^{b\sigma_2}_{a\sigma_1} - (k^A_{a\sigma_1 b\sigma_2} - ik^S_{a\sigma_1 b\sigma_2})E^{a\sigma_1}_{b\sigma_2}, \quad \text{(A13)}$$

$$= \sum_{a\sigma_1>b\sigma 2}\omega_{a\sigma_1 b\sigma_2}E^{b\sigma_2}_{a\sigma_1} - \omega^*_{a\sigma_1 b\sigma_2}E^{a\sigma_1}_{b\sigma_2}, \quad \text{(A14)}$$

$$\hat{\Lambda} = \sum_{i\sigma_1 a\sigma 2}(k^A_{i\sigma_1 a\sigma_2} + ik^S_{i\sigma_1 a\sigma_2})E^{a\sigma_2}_{i\sigma_1} - (k^A_{i\sigma_1 a\sigma_2} - ik^S_{i\sigma_1 a\sigma_2})E^{i\sigma_1}_{a\sigma_2}, \quad \text{(A15)}$$

$$= \sum_{i\sigma_1 a\sigma 2}\lambda_{i\sigma_1 a\sigma_2}E^{a\sigma_2}_{i\sigma_1} - \lambda^*_{i\sigma_1 a\sigma_2}E^{i\sigma_1}_{a\sigma_2}, \quad \text{(A16)}$$

where a, b, c, ... are unoccupied MOs. The matrix $\mathbf{K}$ can be constructed in terms of Λ, Ω^{O}, and Ω^{V} blocks (with diagonal elements Ω^{D}) depending on whether the matrix is spin-blocked or particle-hole blocked,

$$\mathbf{K} = \left[\begin{array}{c|c|c|c} \Omega_{ij} & \Omega_{i\bar{j}} & \Lambda_{ai} & \Lambda_{\bar{a}i} \\ \hline \Omega_{\bar{i}j} & \Omega_{\bar{i}\bar{j}} & \Lambda_{a\bar{i}} & \Lambda_{\bar{a}\bar{i}} \\ \hline \Lambda_{ia} & \Lambda_{\bar{i}a} & \Omega_{ab} & \Omega_{\bar{a}b} \\ \hline \Lambda_{i\bar{a}} & \Lambda_{\bar{i}\bar{a}} & \Omega_{a\bar{b}} & \Omega_{\bar{a}\bar{b}} \end{array}\right] \Leftrightarrow \left[\begin{array}{c|c|c|c} \Omega_{ij} & \Lambda_{ai} & \Omega_{i\bar{j}} & \Lambda_{\bar{a}i} \\ \hline \Lambda_{ia} & \Omega_{ab} & \Lambda_{\bar{i}a} & \Omega_{\bar{a}b} \\ \hline \Omega_{\bar{i}j} & \Lambda_{a\bar{i}} & \Omega_{\bar{i}\bar{j}} & \Lambda_{\bar{a}\bar{i}} \\ \hline \Lambda_{i\bar{a}} & \Omega_{a\bar{b}} & \Lambda_{\bar{i}\bar{a}} & \Omega_{\bar{a}\bar{b}} \end{array}\right], \quad \text{(A17)}$$

where the bar on the index indicates a β MO and its absence indicates an α MO. As demonstrated by Fukutome,[33] the action of Ω^{O} and Ω^{V} blocks leave the Slater determinant $|\Psi\rangle$ invariant up to a phase change, while the Λ block produces a non-trivial change. The equivalence shown in Eq. (A17) is useful as it enables transformation from the particle-hole-blocked form to the spin-blocked form in which our implementation is performed, but where only blocks corresponding to ov generators are of importance.

Equation (A7) can be written in terms of irreducible Cartesian orbital excitation operators,[34]

$$S^{00}_{pq} = (E^p_q + E^{\bar{p}}_{\bar{q}}), \quad \text{(A18)}$$

$$T^x_{pq} = \frac{1}{2}(E^{\bar{p}}_q + E^p_{\bar{q}}), \tag{A19}$$

$$T^y_{pq} = \frac{i}{2}(E^{\bar{p}}_q + E^p_{\bar{q}}), \tag{A20}$$

$$T^z_{pq} = \frac{1}{2}(E^p_q - E^{\bar{p}}_{\bar{q}}), \tag{A21}$$

giving

$$\begin{aligned}\hat{K} = i\sum_p [k^{D,00}_{pp} S^{00}_{pp} + \sum_{x_1,x_2,x_3} k^{D,x_i}_{pp} T^{x_i}_{pp}] + i\sum_{p>q} [k^{S,00}_{pq}(S^{00}_{pq} + S^{00}_{qp}) \\ + \sum_{x_1,x_2,x_3} k^{S,x_i}_{pq}(T^{x_i}_{pq} + T^{x_i}_{qp})] + \sum_{p>q} [k^{A,00}_{pq}(S^{00}_{pq} - S^{00}_{qp}) \\ + \sum_{x_1,x_2,x_3} k^{A,x_i}_{pq}(T^{x_i}_{pq} - T^{x_i}_{qp})].\end{aligned} \tag{A22}$$

APPENDIX B: EXPONENTIAL MAPPING TO THE $SU(2N_{\mathrm{orb}})$ GROUP MANIFOLD

In order to obtain $SU(2N_{\mathrm{orb}})$ group elements from the $\mathfrak{su}(2N_{\mathrm{orb}})$ Lie algebra, exponential mapping from the tangent space to the group manifold is required. Such a procedure can be achieved through the application of Zassenhaus' formula,

$$e^{A+B} = e^A e^B e^{-\frac{1}{2}[A,B]} e^{\frac{1}{6}(2[B,[A,B]]+[A,[A,B]])} e^{\mathcal{O}(N^4)}, \tag{B1}$$

which demonstrates that the exponential mapping back to the group manifold requires the use of the commutators of generators (Table S2). The generators are obtained using the commutator relation of the underlying excitation operators,

$$[E^{q\sigma_2}_{p\sigma_1}, E^{s\sigma_4}_{r\sigma_3}] = \delta_{ps}\delta_{\sigma_1\sigma_4} E^{q\sigma_2}_{r\sigma_3} - \delta_{qr}\delta_{\sigma_2\sigma_3} E^{s\sigma_4}_{p\sigma_1}, \tag{B2}$$

and are found to anticommute (a requirement of a Lie algebra), where the commutator relations demonstrate the subgroup structure (the commutator of two members of a subgroup is also a member of the subgroup).

Truncating Eq. (B1) at second order and using the commutation relation in Eq. (B2) indicate that $[\mathbf{k}_1(p, q), \mathbf{k}_2(r, s)] = \mathbf{k}_3(p, q, r, s)$, where p and q are the non-zero matrix elements in $\mathbf{k}_1$, r and s are the non-zero matrix elements in $\mathbf{k}_2$, and $\mathbf{k}_3$ is the matrix representation of the operator determined by Table S2. There are four terms in $\mathbf{k}_3(p, q, r, s)$, which form a sum of the same generator with different indices $\mathbf{k}_3(p, q, r, s) = \delta_{ps}\mathbf{k}_3(q, r) + \delta_{qr}\mathbf{k}_3(p, s) + \delta_{pr}\mathbf{k}_3(q, s) + \delta_{qs}\mathbf{k}_3(p, r)$. As by definition, the generators $\mathbf{k}_1$ and $\mathbf{k}_2$ have off-diagonal elements, $p \neq q$ and $r \neq s$, and p cannot be equal to both r and s at the same time (with similar relations existing for the other indices); thus, there can only ever be at most two non-zero terms (δ_{ps}, δ_{qr} or δ_{pr}, δ_{qs}). Focusing on the δ_{ps}, δ_{qr} pair (the results are equivalent for the other pair), in the case that $p \neq s$ and $q \neq r$, it is clear that $\mathbf{k}_3 = \mathbf{0}$ owing to Eq. (B2). If $p = s$ and $q = r$, $\mathbf{k}_3 = \mathbf{0}$ if $\hat{k}_3$ is an antisymmetric generator, or has only diagonal elements if it is a symmetric generator (i.e. with elements in Ω^V and Ω^O blocks only) which can be projected as discussed previously. In the case that $p = s$ and $q \neq r$, or that $p \neq s$ and $q = r$, only one of the terms survives and so the second-order terms are obtained from the exponential of a single matrix, rather than a sum that would require reapplication of Eq. (B1). The second order terms involve only rotations in oo or vv blocks but must be retained as due to the action of the first order terms, the orbitals involved are linear combinations of occupied and virtual orbitals. The realization that all terms up to second-order in the exponential mapping are an exponential of a single matrix simplifies generation of the rotated set of MOs.

Exponentiation of a matrix is achieved using the series expansion

$$e^{ik\mathbf{k}} = \sum_{n=0}^{\infty} \frac{1}{n!} i^n k^n \mathbf{k}^n. \tag{B3}$$

Recognizing that $\mathbf{k}^2 = -\mathbf{1}$ for all non-imaginary generators and $i^2\mathbf{k}^2 = -\mathbf{1}$ for all imaginary generators, the exponential is written as

$$e^{k\mathbf{k}} = \mathbf{1}\cos(k) + \mathbf{k}\sin(k), \tag{B4}$$

$$e^{ik\mathbf{k}} = \mathbf{1}\cos(k) + \mathbf{k}i\sin(k), \tag{B5}$$

for real and imaginary generators, respectively. The values of k can be seen to be periodic in the range $(-\pi, \pi]$ (factors of 1/2 are incorporated into k obscuring the underlying 4π periodicity), and as a result of $SU(2N_{\mathrm{orb}})$ being compact and connected, the exponential mapping can be shown to be surjective (many-to-one). Rotations outside the range $(0, \frac{\pi}{2}]$ correspond to trivial phase changes in a group element within the range $(0, \frac{\pi}{2}]$, and so only group elements that lie in the range $(0, \frac{\pi}{2}]$ are required.

[1] C. A. Jiménez-Hoyos, T. M. Henderson, T. Tsuchimochi, and G. Scuseria, J. Chem. Phys. **136**, 164109 (2012).
[2] I. Mayer, Chem. Phys. Lett. **11**, 397 (1971).
[3] P. Pulay and T. P. Hamilton, J. Chem. Phys. **88**, 4926 (1988).
[4] L. M. Thompson and H. P. Hratchian, J. Chem. Phys. **142**, 054106 (2015).
[5] L. M. Thompson and H. P. Hratchian, J. Chem. Phys. **141**, 034108 (2014).
[6] A. J. W. Thom and M. Head-Gordon, Phys. Rev. Lett. **101**, 193001 (2008).
[7] K. Kowalski and K. Jankowski, Phys. Rev. Lett. **81**, 1195 (1998).
[8] H. Fukutome, Prog. Theor. Phys. **52**, 115 (1974).
[9] D. W. Small, E. J. Sundstrom, and M. Head-Gordon, J. Chem. Phys. **142**, 024104 (2015).
[10] C. A. Jiménez-Hoyos, R. Rodríguez-Guzmán, and G. Scuseria, J. Phys. Chem. A **118**, 9925 (2014).
[11] H. B. Schlegel and J. J. W. McDouall, "Do you have SCF stability and convergence problems?," in *Computational Advances in Organic Chemistry: Molecular Structure and Reactivity*, edited by C. Ögretir and I. G. Csizmadia (Kluwer Academic Publishers, Dordrecht, 1991), pp. 167–185.
[12] J. J. Goings, F. Ding, M. J. Frisch, and X. Li, J. Chem. Phys. **142**, 154109 (2015).
[13] Z. Tóth and P. Pulay, J. Chem. Phys. **145**, 164102 (2016).
[14] L. M. Thompson and H. P. Hratchian, J. Phys. Chem. A **119**, 8744 (2015).
[15] L. M. Thompson, C. C. Jarrold, and H. P. Hratchian, J. Chem. Phys. **146**, 104301 (2017).
[16] K. T. Jensen, R. L. Benson, S. Cardamone, and A. J. W. Thom, J. Chem. Theory Comput. **14**, 4629 (2018).
[17] L. C. Jake, T. M. Henderson, and G. Scuseria, J. Chem. Phys. **148**, 024109 (2018).
[18] K. J. Oosterbaan, A. F. White, and M. Head-Gordon, J. Chem. Phys. **149**, 044116 (2018).
[19] H. Fukutome, Prog. Theor. Phys. **45**, 1382 (1971).
[20] D. J. Thouless, Nucl. Phys. **21**, 225 (1960).
[21] J. L. Stuber and J. Paldus, "Symmetry breaking in the independent particle model," in *Fundamental World of Quantum Chemistry: A Tribute to the Memory of Per-Olov Löwdin*, edited by E. Brandas and E. S. Kryachko (Kluwer Academic Publishers, 2003), pp. 67–140.
[22] A. Yershova, S. Jain, S. M. LaValle, and J. C. Mitchell, Int. J. Rob. Res. **29**, 801 (2010).

[23]J. C. Mitchell, SIAM J. Sci. Comput. **30**, 525 (2008).
[24]F. Neese, J. Phys. Chem. Solids **65**, 781 (2004).
[25]G. M. J. Barca, A. T. B. Gilbert, and P. M. W. Gill, J. Chem. Theory Comput. **14**, 1501 (2018).
[26]L. M. Thompson, X. Sheng, A. Mahler, D. Mullally, and H. P. Hratchian (2018). "MQCpack v0.1-beta," Zenodo.
[27]M. J. Frisch, G. W. Trucks, H. B. Schlegel, G. E. Scuseria, M. A. Robb, J. R. Cheeseman, G. Scalmani, V. Barone, G. A. Petersson, H. Nakatsuji, X. Li, M. Caricato, A. V. Marenich, J. Bloino, B. G. Janesko, R. Gomperts, B. Mennucci, H. P. Hratchian, J. V. Ortiz, A. F. Izmaylov, J. L. Sonnenberg, D. Williams-Young, F. Ding, F. Lipparini, F. Egidi, J. Goings, B. Peng, A. Petrone, T. Henderson, D. Ranasinghe, V. G. Zakrzewski, J. Gao, N. Rega, G. Zheng, W. Liang, M. Hada, M. Ehara, K. Toyota, R. Fukuda, J. Hasegawa, M. Ishida, T. Nakajima, Y. Honda, O. Kitao, H. Nakai, T. Vreven, K. Throssell, J. A. Montgomery, Jr., J. E. Peralta, F. Ogliaro, M. J. Bearpark, J. J. Heyd, E. N. Brothers, K. N. Kudin, V. N. Staroverov, T. A. Keith, R. Kobayashi, J. Normand, K. Raghavachari, A. P. Rendell, J. C. Burant, S. S. Iyengar, J. Tomasi, M. Cossi, J. M. Millam, M. Klene, C. Adamo, R. Cammi, J. W. Ochterski, R. L. Martin, K. Morokuma, O. Farkas, J. B. Foresman, and D. J. Fox, GAUSSIAN 16, Revision A.03, Gaussian, Inc., Wallingford, CT, 2016.
[28]S. Huzinaga, J. Chem. Phys. **42**, 1293 (1965).
[29]T. M. Henderson, C. A. Jiménez-Hoyos, and G. Scuseria, J. Chem. Theory Comput. **14**, 649 (2018).
[30]D. J. Wales and J. P. K. Doye, J. Phys. Chem. A **101**, 5111 (1997).
[31]J. Paldus, J. Chem. Phys. **61**, 5321 (1974).
[32]M. V. Berry, Proc. R. Soc. A **392**, 45 (1984).
[33]H. Fukutome, Int. J. Quantum Chem. **20**, 955 (1981).
[34]T. Helgaker, P. Jørgensen, and J. Olsen, *Molecular Electronic-Structure Theory* (Wiley, 2012).